THE JOURNAL OF PHYSICAL CHEMISTRY Letters

Letter

pubs.acs.org/JPCL

Automated Discovery and Construction of Surface Phase Diagrams Using Machine Learning

Zachary W. Ulissi, Aayush R. Singh, Charlie Tsai, and Jens K. Nørskov*

SUNCAT Center for Interface Science and Catalysis, Department of Chemical Engineering, Stanford University, Stanford, California 94305, USA

SUNCAT Center for Interface Science and Catalysis, SLAC National Accelerator Laboratory, Menlo Park, California 94025, USA

Supporting Information

ABSTRACT: Surface phase diagrams are necessary for understanding surface chemistry in electrochemical catalysis, where a range of adsorbates and coverages exist at varying applied potentials. These diagrams are typically constructed using intuition, which risks missing complex coverages and configurations at potentials of interest. More accurate cluster expansion methods are often difficult to implement quickly for new surfaces. We adopt a machine learning approach to rectify both issues. Using a Gaussian process regression model, the free energy of all possible adsorbate coverages for surfaces is predicted for a finite number of adsorption sites. Our result demonstrates a rational, simple, and systematic approach for generating accurate free-energy diagrams with reduced computational resources. The Pourbaix diagram for the $IrO_2(110)$ surface (with nine coverages from fully hydrogenated to fully oxygenated surfaces) is reconstructed using just 20 electronic structure relaxations, compared to approximately 90 using typical search methods. Similar efficiency is demonstrated for the MoS_2 surface.

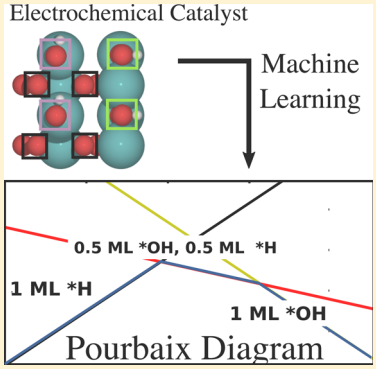

The construction of free-energy diagrams for reactions on heterogeneous surfaces is central for understanding catalysts and for designing new ones. The free energies of individual adsorbates relative to the gas phase are necessarily dependent on their surface coverages due to adsorbate−adsorbate interactions. For each set of proposed reaction conditions, it is necessary to estimate the thermodynamic surface coverage of each species in order to construct an accurate free-energy diagram. Although there is an ensemble of possible surface coverages for a given set of conditions, it is common to approximate the surface configuration as a static configuration with the lowest free energy. These configurations are usually mapped out and illustrated using surface phase diagrams that plot the free energy of each configuration as a function of applied potential and possibly other environmental parameters such as gas-phase fugacities or pH. The most common form of these surface phase diagrams in electrochemistry is the Pourbaix diagram, where the phases are mapped as a function of applied potential and pH. The construction of these diagrams is a computationally intensive process and often performed by researchers using ad hoc exploration methods. This process typically involves calculations of the surface energies for a few adsorbate configurations, chosen using the researcher's physical intuition or based on experimental findings. More accurate methods to solve this problem exactly such as cluster expansion methods[1−3] are often eschewed due to the complexity of implementing these procedures for arbitrary surfaces and because the workflow is usually not compatible with results from ad hoc exploration-based approaches.

To illustrate the typical construction of these surface phase diagrams, we consider two experimentally relevant heterogeneous electrochemical catalysts: a unit cell of the (110) iridium oxide (IrO_2) surface (illustrated in Figure 1A) and a four-site edge of sulfur-exposed molybdenum disulfide (MoS_2) stripe.[4,5] Both of these surfaces have been considered for the electrochemical hydrogen evolution reaction (HER) and the reduction of N_2 to ammonia. We focus on the ammonia synthesis reaction here because it involves large applied potentials and hence a large range of possible adsorbates and configurations. We started with a large number of electronic energies, calculated using density functional theory (DFT), for various surface coverages that had been constructed by picking likely structures based on intuition (MoS_2, 56 coverages[4,5]) or through a sequential search of progressively reduced structures (IrO_2, 93 structures), described in the Supporting Information. For the experimentally relevant conditions of applied potentials between −1.5 and 0.0 V vs RHE (the reversible hydrogen electrode), both structures transition from oxidized states at approximately 0 V (primarily hydroxyl adsorbates) to reduced states at approximately −1 V (primarily hydrogenated surfaces), with mixed coverages at around −0.5 V. Both data sets represent relatively thorough searches of the configuration space using considerable computational resources (approximately 200 DFT relaxations for different coverages and different configurations at each coverage). Despite this

Received: June 8, 2016
Accepted: August 24, 2016
Published: August 24, 2016

DOI: 10.1021/acs.jpclett.6b01254
J. Phys. Chem. Lett. 2016, 7, 3931−3935

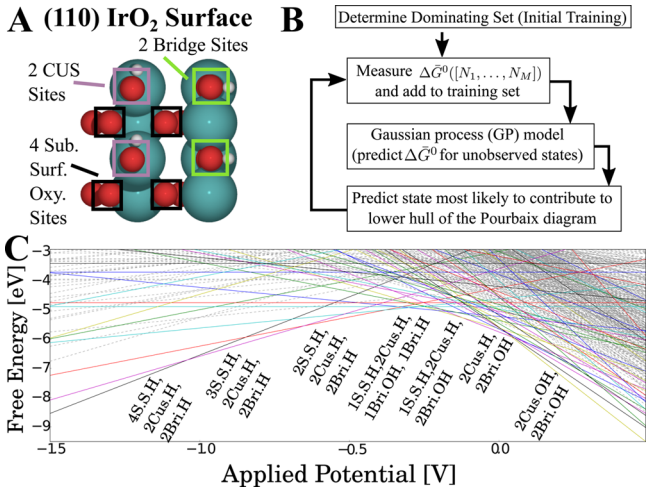

Figure 1. Demonstration of Pourbaix diagram construction for an IrO_2 surface. (A) Illustration of the three types of adsorption sites considered for a 2 × 2 IrO_2 slab. (B) Algorithm for Pourbaix diagram construction using a machine learning model to guide simulation choice. (C) Final Pourbaix diagram, with the states forming the lower hull labeled. Dashed lines are those predicted for unmeasured configurations.

considerable investment of resources, there were several outstanding questions that we consider in this work:

1. What is the probability that we have discovered the complete set of coverages that form the lower hull of the surface−adsorbate phase diagram? Conversely, what is the probability that we have missed minimal states?
2. How many evaluations are required to efficiently explore the surface phase diagram? Are there procedures to more efficiently explore the entire space and save computational resources?

In this work, we present a machine learning (ML) approach for generating approximate Pourbaix diagrams for all possible surface coverages using the free energies for a small number of configurations calculated using DFT. We show that a ML approach based on Gaussian process (GP) regression efficiently reproduces free energies from the training data set and predicts the free energies of previously unconsidered surface coverage configurations along with empirically verified estimates of the prediction uncertainty. Using this approach, we provide estimates of the probability that a given set of surface coverages contains the configurations that form the lower hull of the Pourbaix diagram. Further, we estimate the likelihood that each unobserved state may contribute to this lower hull, providing the most likely candidates for further computational experiments and forming the basis for a more efficient strategy for choosing necessary computations. For the two example surfaces of MoS_2 and IrO_2, the developed strategies reproduce the experimentally relevant lower hull of the Pourbaix diagram using only ∼20−30 DFT relaxations for various coverages, compared to ∼60−90 relaxations using ad hoc exploration methods. Further, these methods revealed surface coverages having the minimum free energy at intermediate applied potentials that the ad hoc exploration methods had missed.

The sheer number of mixed-coverage surface phases drives the complexity of constructing surface phase diagrams. For example, the 2 × 2 IrO_2 surface, illustrated in Figure 1A, contains eight possible adsorption sites. There are two coordinatively unsaturated (cus) surface sites, two bridge sites, and four subsurface oxygens that can adsorb hydrogens. For the cus and bridge sites, we consider four possible states (*, *OH, *H, *O), while the subsurface oxygens have two states (*O, *OH). The number of unique adsorbate configurations for this surface is 4096, before taking into account rotational, translational, and mirror symmetries. The mean-field configurations are states corresponding to discrete surface coverages without considering the precise arrangement of the adsorbates on the surface. Each mean-field configuration maps to several possible configurations, so that the number of mean-field configurations is substantially smaller than the number of unique adsorbate configurations. The number of mean-field configurations for the 2 × 2 IrO_2 surface is 500, substantially lower than the number of unique configurations but still a large number of states to consider for inclusion in the final phase diagram. Likewise, for the example of a four-site MoS_2 edge, illustrated in the Supporting Information, each site has one of six possible states (vacancy *, *OH, *H_2, *H, *NNH, *N_2), and there are 1296 unique configurations (before symmetry reduction) and 126 unique coverage or mean-field configurations. The number of mean-field configurations in each of these cases can be derived analytically using the weak composition function, as shown in the Supporting Information. In both cases, the number of possible states increases quickly with system size; therefore, this reduction becomes more important for large surfaces with many adsorption sites.

For these examples and many others in electrochemistry with small adsorbates, the mean-field coverage is a reasonable approximation to the energy of each possible configuration at that coverage.[6] For the IrO_2 surface, the potential energy of several possible adsorbate configurations for 16 unique coverages was calculated using explicit DFT relaxations, as shown in the Supporting Information. For example, a surface with just two CO adsorbates could have the CO molecules adjacent on the cus site, adjacent on the bridge site, or diagonal. At most coverages, the error in mapping from unique adsorbate configurations to coverages, defined as the difference between the energy of the highest-energy configuration and the energy of the lowest-energy configuration at identical coverages, was under 0.1 eV, and the average of this error for all coverages was 0.14 eV. This error tended to be larger at high surface coverages and with bulkier adsorbates like *OH and even in the worst cases was less than 0.6 eV. Identifying the minimum-energy configuration at a given coverage is a well-addressed problem in computational surface science and can be accomplished either with physical intuition and multiple trials for simple configurations or using established techniques like a constrained minima hopping algorithm[7] for global optimization of the potential energy with respect to adsorbate positions. For this study, the lowest-energy configurations were found through physical intuition and multiple adsorbate configuration trials.

A surface phase diagram in electrochemistry is constructed by identifying the phase with the lowest free energy at each set of imposed reaction reactions, usually as a function of the applied potential and other environmental conditions (pH, gas-phase pressures, etc.). The details of the electrochemical free energy are included in the Supporting Information. A surface phase with a given coverage can be excluded from the phase diagram if we can predict with confidence that its free energy lies significantly above the lowest free-energy configurations at all reaction conditions, as illustrated in Figure 1C. Most states in the surface phase diagram are more than 1 eV higher than the minimum-energy configuration (the lower hull of the phase

DOI: 10.1021/acs.jpclett.6b01254
J. Phys. Chem. Lett. 2016, 7, 3931−3935

diagram). Therefore, we can reasonably exclude these states from the phase diagram without doing explicit DFT relaxations if we can predict the free energy of that state with precision better than 1 eV. This is a relatively easy standard to meet without the use of more sophisticated methods like cluster expansion methods.[1−3] We have found that a simple GP regression scheme to predict the free energy of a state with only species' surface coverages as a feature vector is sufficient to quickly determine which surface phases will likely contribute to the final phase diagram. This process is simple, efficient, and does not require significant insight into the possible configurations on a surface as it is simply based on mean-field coverages. Furthermore, the Bayesian nature of the GP model makes tracking uncertainty in predictions straightforward.

We estimate the coverage-dependent free energy of each mean-field configuration using a ML approach based on GP regression. The GP model was chosen for its advantageous properties for online optimization and feedback, primarily its ability to provide uncertainty estimates for the free energies of unknown states. We chose the fingerprint for each state as the fractional coverage of each surface species $[x_1,..., x_n]$. The uncertainty in the GP regression increases with the distance in coverage space, that is, predictions for an unmeasured configuration are more reliable when similar to a configuration that we have already measured with full DFT accuracy. For the training set in the GP, we assume an uncertainty in each free-energy DFT relaxation of 0.1 eV (see the Computational Methods for details of the calculations). This error incorporates uncertainty in the underlying DFT relaxation as well as uncertainty that the configuration is the lowest-energy configuration for the specified mean-field coverage, as described above. However, this assumed uncertainty has no impact on the final results as all configurations in the final phase diagram will have been studied with full DFT accuracy. This uncertainty is instead used to help in the fitting of the GP. We observe that the uncertainty estimates from the GP when trained against a small set of known free energies and used to predict a set of known free energies compare reasonably with the actual error between the predictions and the known values. A GP trained on the free energies of just a few surface phases will make predictions with large uncertainty. As the most likely surface phases are examined with DFT calculations and added to the training set, the accuracy of predictions will improve, as illustrated in the parity plots included in the Supporting Information. It is acceptable for the GP uncertainty for configurations not in the final phase diagram to be significantly larger than 0.1 eV, as long as the energy of that state lies far above minimum-energy configurations.

For a new surface for which no DFT energetics are available, an initial training set is chosen that spans the input coverage feature space. To evenly cover this space, we choose a dominating subset of the graph, that is, a subset of nodes on the graph such that every node not in the subset is no more than one vertex away from a node in the subset, as illustrated in Figure 2B. The goal of this process is to evenly cover the entire network, as illustrated in Figure 2B. If the dominating set contains more than approximately one node per dimension, we instead choose dominating sets such that every node is within two or three vertexes of a node in the dominating set. For example, the dominating set of the configuration space for the IrO_2 example contains approximately 90 nodes. Instead, we choose a dominating subset of nodes within three links of every node on the graph, resulting in just nine nodes evenly spread across across coverage space. For comparison, the points chosen through the progressive search method described in the Supporting Information are shown in Figure 2A. This process results in a training set for the GP that will yield reasonable predictions for most coverages because all coverages will be quite close in coverage space to one of these points. In many cases, we have found that this initial training set is sufficient to predict most of the coverages that will contribute to the final surface phase diagram.

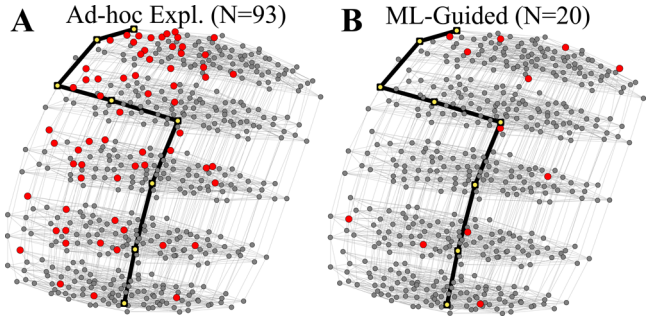

Figure 2. Visualization of the network of possible surface configurations for IrO_2 and the exploration process described in this work. Light gray connections indicate surface coverages that differ by a single adsorbate (changing one adsorbate to another type or adding/removing a single adsorbate) and illustrate the distance in the feature space. Islands in the feature space arise based on the number of subsurface hydrogens adsorbed (0−5). (A) Possible states of the IrO_2 system (500 configurations, gray). Connected yellow points are those that form the lower hull of the Pourbaix diagram, all of which were sampled explicitly with DFT. Red points are those sampled using a typical intuition-based exploration method. All points in the lower hull were sampled explicitly with DFT. (B) Points sampled by the ML-guided effort that identified the lower hull of the Pourbaix diagram using just 20 DFT relaxations, starting with the dominating set for initial point selection.

Once a number of configurations are available as a training set for the GP, either by using DFT energetics from previous ad hoc studies or through the dominating set method described above, the GP model is refined in an iterative fashion by choosing configurations likely to contribute to the phase diagram and adding those configurations to the training set. This feedback process is illustrated in Figure 1B. New configurations are chosen for DFT study based on the probability of contributing to the lower hull, based on the GP-estimated energies and uncertainties. These configurations are studied with full DFT accuracy, which involves several DFT relaxations to identify the lowest-energy configuration at the specified coverage. The lowest-energy configuration is then added to the training set of coverage to energy mappings. This GP-based prediction scheme for a sample phase diagram is illustrated in Figure 3. Starting with a number of states that have been measured with full DFT accuracy and currently contribute to the surface phase diagram (the lower hull), predictions are made for two trial coverages that could be chosen for study. The first unmeasured coverage is predicted to lie far above the lower hull and can be safely excluded from further study despite considerable (1 eV) uncertainty in the predicted free energy. The second unmeasured coverage is predicted to possibly cross the lower hull at approximately 0.7 eV and will be chosen for full DFT study. The final phase diagram will consist entirely of states that have been measured

DOI: 10.1021/acs.jpclett.6b01254
J. Phys. Chem. Lett. 2016, 7, 3931−3935

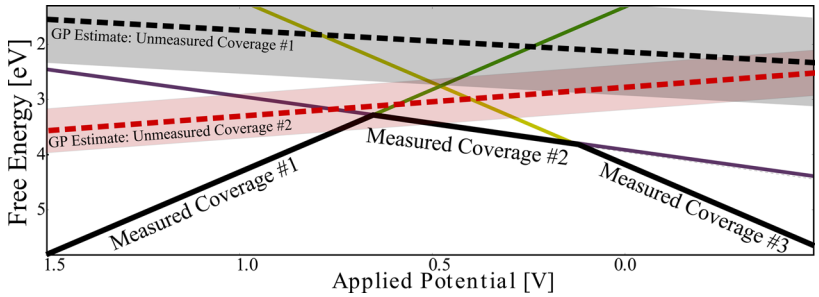

Figure 3. Illustration of the GP-based prediction scheme for choosing coverages to study with full DFT accuracy. Solid colored lines are states that have previously been studied with DFT, and the solid black line is the lower hull (the current best estimate of states in the surface phase diagram). Dashed lines are GP predictions for coverages, with shaded regions representing uncertainty in the GP estimate. Unmeasured coverage #2 is likely to contribute to the lower hull and will be studied with DFT. Unmeasured coverage #1 is very unlikely to contribute to the final phase diagram, despite being a prediction with large uncertainty, and can safely be neglected in DFT studies.

with full DFT accuracy; therefore, no precision is lost in the final result.

We find that this process usually results in the complete set of states that form the lower hull of the Pourbaix diagram within approximately 20 steps, as illustrated in Figure 4 for the

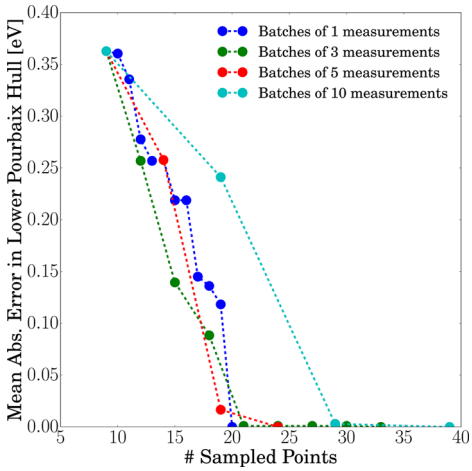

Figure 4. Convergence of the estimated lower hull of the IrO_2 Pourbaix diagram. All points start with the same set of initial points chosen by establishing a dominating set of the feature space. Batches of the most likely configurations to sample and sampling continue until the true lower Pourbaix hull is recovered.

IrO_2 example. Choosing batches of configurations to sample allows for a more efficient exploration because configurations can be measured in parallel on modern computing clusters but results in more total evaluations because the GP model is updated less frequently. The convergence of these methods is shown in Figure 4. Batches of five configuration measurements represent a reasonable amount of parallelism while only requiring four more total measurements to find the final hull. All batch sizes start from the same set of initial measurements chosen through the dominating set method, as outlined above. Using this scheme, eight coverages are found to contribute to the final phase diagram, ranging from a fully hydrogenated surface at applied potentials less than −1 V to mixed H/OH/vacancy phases at around [−1 V, 0.0 V] and fully hydroxyl covered surfaces at potentials more positive than 0.0 V. Examples of mixed-coverage phases include partial monolayers of hydrogen (hydrogens on bridge and cus sites but varying numbers in the subsurface) and mixed coverages of hydroxyl and hydrogen coverage. We find that there are no potential regions at these conditions where adsorbed oxygen (not hydroxyl) is stable on the surface. Oxygen coverage begins at significantly more positive applied potentials.

This approach can easily be extended to more general phase diagrams including environmental conditions such as pH, temperature, and reactant-free species potentials. Most of these parameters will simply affect the adsorbate corrections $f_i(T,P)$. Constructing phase diagrams with more than one parameter is also possible, though the process of identifying $(T,P,U)^{\min}$ and the corresponding probability of crossing the lower hull becomes computationally more expensive.

Learning methods such as the GP model illustrated herein can significantly reduce the complexity involved in constructing surface phase diagrams for new surfaces and enable the identification of regions with relevant mixtures of adsorbates. These regions of interests are typically at moderate applied potentials, where the surface is neither fully oxidized nor reduced. For reactions where key surface intermediates are expected to be present in small amounts, the correct identification of these configurations is crucial. Typical approaches in the literature involve selecting a few representative coverages (usually full monolayers or simple fractional coverages) due to the complexity and computational cost of identifying optimal coverages at each potential. This work shows that at typical operating conditions for many common reactions, such as the HER (between −0.3 and 0 V vs RHE), the surface coverage may be quite different from simply monolayers. Due to the presence of adsorbate−adsorbate interactions, the complex surface coverages identified with our approach can also help improve the estimates of reaction free-energy diagrams.

■ COMPUTATIONAL METHODS

Electronic structure relaxations were performed using the Quantum Espresso software package[8] implemented in the Atomic Simulation Environment (ASE).[9] The BEEF−vdW exchange−correlation functional[10] was used to accurately model adsorption energies, taking into account van der Waals interactions. Calculations for IrO_2 were conducted on $2 \times 2 \times 4$ slabs of the (110) facet of the rutile oxide crystal structure (space group: $P4_2/mnm$), with 10 Å of vacuum in the z-direction. Adsorbates and the upper two layers were relaxed such that the maximum force on each atom was less than 0.05 eV/Å. The plane wave and density wave cutoffs were 500 and

DOI: 10.1021/acs.jpclett.6b01254
J. Phys. Chem. Lett. 2016, 7, 3931−3935

5000 eV, respectively, and k-point sampling was implemented using a 4 × 4 × 1 Monkhorst−Pack grid.

DFT adsorption energies were calculated relative to gas-phase H_2O and H_2. Free-energy corrections were applied to the DFT energy at T = 300 K and P = 1 bar, using the ideal gas approximation for gas-phase species and the harmonic approximation for adsorbates. The per-adsorbate corrections including enthalpy, entropy, and zero-point energy were found to be +0.20 eV for *H, +0.35 eV for *OH, and +0.05 eV for *O. These corrections were assumed to apply to all configurations, though small differences in the vibrational states of adsorbates in different configurations could be possible.

Reported DFT energies for each mean-field coverage are the energies of the lowest-energy configuration for a given coverage. Several possible configurations were generally attempted for each coverage to identify the configuration with the lowest energy. For example, in this work with relatively small adsorbates, different configurations at the same coverage generally had quite similar energies (within approximately 0.1 eV), as shown in the Supporting Information, and had a small effect on the final diagrams.

■ ASSOCIATED CONTENT

Supporting Information

The Supporting Information is available free of charge on the ACS Publications website at DOI: 10.1021/acs.jpclett.6b01254.

Results that show the applicability of the mean-field approximation, mathematical details about the derivation of the number of mean-field sites for arbitrary surfaces, the thermodynamic treatment of the electrochemical free energy, and the method used to identify the most likely coverages, applications of these methods to a second example, MoS_2 edges, and the final resulting Pourbaix diagram, network structure, and search convergence (PDF)

■ AUTHOR INFORMATION

Corresponding Author

*E-mail: norskov@stanford.edu. Phone: (650) 723-8487.

Notes

The authors declare no competing financial interest.

■ ACKNOWLEDGMENTS

The authors acknowledge financial support from the U.S. Department of Energy Office of Basic Sciences to the SUNCAT Center for Interface Science and Catalysis. C.T. acknowledges financial support from the U.S. National Science Foundation Graduate Research Fellowship Program.

■ REFERENCES

(1) Kitchin, J. R.; Reuter, K.; Scheffler, M. Alloy surface segregation in reactive environments: first-principles atomistic thermodynamics study of Ag 3 Pd (111) in oxygen atmospheres. *Phys. Rev. B: Condens. Matter Mater. Phys.* **2008**, *77*, 075437.

(2) Tang, H.; Van der Ven, A.; Trout, B. L. Phase diagram of oxygen adsorbed on platinum (111) by first-principles investigation. *Phys. Rev. B: Condens. Matter Mater. Phys.* **2004**, *70*, 045420.

(3) Lerch, D.; Wieckhorst, O.; Hammer, L.; Heinz, K.; Müller, S. Adsorbate cluster expansion for an arbitrary number of inequivalent sites. *Phys. Rev. B: Condens. Matter Mater. Phys.* **2008**, *78*, 121405.

(4) Tsai, C.; Abild-Pedersen, F.; Nørskov, J. K. Tuning the MoS2 edge-site activity for hydrogen evolution via support interactions. *Nano Lett.* **2014**, *14*, 1381−1387.

(5) Tsai, C.; Chan, K.; Abild-Pedersen, F.; Nørskov, J. K. Active edge sites in MoSe2 and WSe2 catalysts for the hydrogen evolution reaction: a density functional study. *Phys. Chem. Chem. Phys.* **2014**, *16*, 13156−13164.

(6) Hansen, H. A.; Rossmeisl, J.; Nørskov, J. K. Surface Pourbaix diagrams and oxygen reduction activity of Pt, Ag and Ni(111) surfaces studied by DFT. *Phys. Chem. Chem. Phys.* **2008**, *10*, 3722−3730.

(7) Goedecker, S. Minima hopping: an efficient search method for the global minimum of the potential energy surface of complex molecular systems. *J. Chem. Phys.* **2004**, *120*, 9911−9917.

(8) Giannozzi, P.; Baroni, S.; Bonini, N.; Calandra, M.; Car, R.; Cavazzoni, C.; Ceresoli, D.; Chiarotti, G. L.; Cococcioni, M.; Dabo, I.; et al. QUANTUM ESPRESSO: a modular and open-source software project for quantum simulations of materials. *J. Phys.: Condens. Matter* **2009**, *21*, 395502.

(9) Bahn, S. R.; Jacobsen, K. W. An object-oriented scripting interface to a legacy electronic structure code. *Comput. Sci. Eng.* **2002**, *4*, 56−66.

(10) Wellendorff, J.; Lundgaard, K. T.; Møgelhøj, A.; Petzold, V.; Landis, D. D.; Nørskov, J. K.; Bligaard, T.; Jacobsen, K. W. Density functionals for surface science: Exchange-correlation model development with Bayesian error estimation. *Phys. Rev. B: Condens. Matter Mater. Phys.* **2012**, *85*, 235149.

DOI: 10.1021/acs.jpclett.6b01254
J. Phys. Chem. Lett. 2016, 7, 3931−3935